IIETA International Information and Engineering Technology Association
Advancing the World of Information and Engineering

Annales de Chimie - Science des Matériaux
Vol. 50, No. 3, June, 2026, pp. 253-260
Journal homepage: http://iieta.org/journals/acsm

Mechanical Performance, Durability, and Microstructural Characterization of Sustainable Geopolymer Mortar Incorporating Fly Ash and GGBS

K. Rama Krishna Reddy*, D. Rajkumar

Civil & Structural Engineering Department, Faculty of Engineering and Technology, Annamalai University, Annamalainagar 608002, India

Corresponding Author Email: k.ramakrishnareddy3949@gmail.com

Copyright: ©2026 The authors. This article is published by IIETA and is licensed under the CC BY 4.0 license (http://creativecommons.org/licenses/by/4.0/).

https://doi.org/10.18280/acsm.500305

Received: 12 April 2026
Revised: 10 June 2026
Accepted: 17 June 2026
Available online: 30 June 2026

Keywords:
geopolymer mortar, compressive strength, split tensile strength, water absorption, rapid chloride permeability test, X-ray diffraction, scanning electron microscopy

ABSTRACT

The research analyzes the geopolymer mortar that results from substituting cement with fly ash (FA), ground granulated blast furnace slag (GGBS), and 50/50 FA-GGBS combination (F50G50). The mechanical, durability, and microstructural characteristics are determined through compressive and tensile strength tests, water absorption and rapid chloride permeability test (RCPT), and the X-ray diffraction (XRD), scanning electron microscopy (SEM), and energy-dispersive spectroscopy (EDS) analysis. Findings revealed that all samples had higher performance than the conventional cement mortar. F50G50 mixture recorded maximum compressive and split tensile strength values of 46.19 MPa and 4.85 MPa after 90 days, which is 19.91% and 32.88% greater than those obtained in the control sample. Reduction in water absorption was about 38% and chloride permeability by 63%, which implies that the durability of such material increased. The XRD analysis revealed geopolymer materials along with quartz, mullite, and minerals containing calcium elements. SEM analysis revealed that the sample consisted of dense and uniform matrix structure with reduced pores and cracks while EDS analysis revealed dominant Si, Al, and O elements along with some amounts of Ca suggesting sodium aluminosilicate hydrate (N-A-S-H) and calcium aluminosilicate hydrate (C-A-S-H) gels.

1. INTRODUCTION

The increasing development of worldwide construction industries has led to enormous consumption of ordinary Portland cement (OPC), which is one of the most common materials in the field [1-3]. However, manufacturing OPC entails a lot of energy consumption and produces large amounts of CO_2 (about 8%), mostly caused by limestone calcination and burning of fuels when manufacturing clinker [4-6]. Also, the extraction of raw materials causes depletion of non-renewable natural resources and ecological damage. Thus, the creation of sustainable cement alternatives is considered to be one of the highest-priority tasks in civil engineering [7].

One of such alternatives is geopolymer concrete (GPC), which has proven to provide various advantages compared to OPC in environmental and engineering terms. Instead of Portland cement, it uses aluminosilicate raw materials with high concentrations of SiO_2 and Al_2O_3, which polymerize in the presence of alkaline agents and create three-dimensional inorganic structure, which is characterized by high strength and durability. Geopolymerization leads to the reduction in greenhouse gases and allows reusing industrial wastes [8-10].

The aluminosilicate material used in the creation of geopolymers is class F fly ash (FA) and ground granulated blast furnace slag (GGBS). The former is highly rich in reactive Si and Al. However, its reaction rate is relatively slow and requires elevated temperature for the achievement of early strength, which reduces the opportunities for its usage in cast-in-situ concreting. GGBS contains CaO in addition to Si and Al, which accelerates the process of geopolymerization and creates sodium aluminosilicate hydrate (C-A-S-H) and calcium aluminosilicate hydrate (N-A-S-H) gels, improving early strength and enabling ambient curing [11-13].

In general, mixing FA and GGBS as a complete cement alternative is widely studied nowadays. The synergetic effects provided by both components allow improving reaction rates, matrix densification, porosity, and mechanical properties. In particular, FA ensures high strength and improved workability due to spherical particles, whereas GGBS increases setting time and promotes early strength due to matrix tightening. The optimal FA: GGBS ratio becomes crucial for achieving desirable fresh properties and mechanical characteristics [14].

The assessment of mechanical properties is important for ensuring reliable performance of concrete in constructional use. High compressive, split tensile, and flexural strengths of geopolymers based on FA and GGBS may be observed due to the denser matrix, lower porosity, and higher bond strength between binder and aggregates. Moreover, the content of Ca in the product further improves matrix density [15].

Durability in severe conditions is an important requirement in construction. GPC demonstrates low water absorption,

sorptivity, chloride penetration, and sulfate and acid resistance as well as resistance to rapid chloride penetration and high temperature, due to the dense microstructure. These properties make the developed GPC a good choice for the construction of marine structures, industrial floors, wastewater treatment plants, and transport infrastructure [16].

For the analysis of reactions and mechanisms, the microstructural analysis of the material should be conducted. The analysis of the material's mineral composition and phase transformation is performed with the help of X-ray diffraction analysis (XRD). Its results allow observing changes in peaks that indicate decreasing crystalline minerals and increasing of amorphous gels. GGBS facilitates the appearance of calcium-containing compounds, which increases strength and durability [17].

The evaluation of mineralogy is complemented by scanning electron microscopy (SEM), which allows analyzing the shape and structure of pores, as well as unreacted particles and microcracks and studying the interfacial transition zone. Energy-dispersive spectroscopy (EDS) is used in combination with SEM for investigating the distribution and ratios of elements (Si, Al, Ca, Na, O, etc.) [18].

This investigation assesses the mechanical properties and durability of the geopolymer mortar by testing and analysis, and studies the microstructure of the material using XRD, SEM, and EDS techniques. The findings will help gain insight into the correlation between the microstructure of geopolymer mortars and their mechanical performance.

2. MATERIALS

For this study, both byproducts and natural aggregates were used to obtain GPC. OPC 53 grade (IS 12269:2013 [19]) was initially subjected to testing purposes but was totally substituted with Class F FA and GGBS in geopolymer mixes. OPC had specific gravity (SG) of 3.12, standard consistency of 32% and 90 μm particle size. Class F FA (Ramagundam Power Plant, IS 3812 (Part 1):2013 [20]) had SG of 2.18 and fineness of 6422 cm²/g. GGBS (ASTM C989 [21]) was added as aluminosilicate raw material to promote the process of geopolymerization and enhance early strength. For fine aggregate, Zone II River sand according to IS 383:2016 [22] was used. Its bulk density was 1.41 g/cm³, SG 2.68 and fineness modulus 2.9. Polycarboxylate ether-based superplasticizer, Armix Hyyecrete PC 20 (IS 9103:2004 [23]) was used to increase concrete workability, where its optimal content was established through initial experiments. Alkaline activator included both NaOH and Na_2SiO_3 with Na_2SiO_3/NaOH ratio of 2.5. In laboratory conditions 12 M NaOH solution was obtained using commercial flakes in distilled water, while commercially available Na_2SiO_3 solution was applied as such.

3. MIX PROPORTION

A control mixture with a cement-to-sand ratio of 1:3 was chosen as the basis for comparison. Three types of GPC mixtures were made using a complete replacement of cement with FA and GGBS in different percentages. The first mixture was made up of 100% FA (724.12 kg/m³), the second of 100% GGBS (724.12 kg/m³), and the third mixture included equal amounts of both FA and GGBS, i.e., 362.06 kg/m³ each, which gave a constant total binder volume of 724.12 kg/m³. Sand was used in the same volume in all three geopolymer mixtures 1086.20 kg/m³. The alkaline activator mixture was made up of NaOH and Na_2SiO_3 in a constant ratio. The amount of Na_2SiO_3 and NaOH used was 206.89 kg/m³ and 82.76 kg/m³, respectively, giving a total volume of the alkaline liquid of 289.65 kg/m³. The ratio of Na_2SiO_3 to NaOH was 2.5, and the amount of water used in all GPC mixtures was 72.41 kg/m³. The mix proportions adopted for the geopolymer mortar and OPC control mortar are presented in Table 1.

Table 1. Mix proportion of mortar specimens

Cementitious Material	FA (kg/m³)	GGBS (kg/m³)	Sand (kg/m³)	NaOH (kg/m³)	Na_2SiO_3 (kg/m³)	Alkaline Liquid (kg/m³)	Water (kg/m³)	Na_2SiO_3/NaOH
FA 100%	724.12	–	1086.20	82.76	206.89	289.65	72.41	2.5
GGBS 100%	–	724.12	1086.20	82.76	206.89	289.65	72.41	2.5
FA50% + GGBS50%	362.06	362.06	1086.20	82.76	206.89	289.65	72.41	2.5
C100% (OPC Control)	Cement : Sand = 1 : 3							

Note: FA = fly ash; GGBS = ground granulated blast furnace slag; OPC = ordinary Portland cement.

4. METHODS

A comprehensive experimental procedure was adopted to study the mechanical, durability, and microstructure of GPC. Compression test was conducted on 150mm cube specimens after 7 days, 28 days and 90 days curing, as per IS 516 (Part 1/Sec 1):2021 [24], using calibrated compression testing machine, where average values from three samples were used for each mix. Splitting tensile strength test was carried out using circular samples of 150 mm and 300 mm of diameter and height according to IS 5816:1999 [25], which involved diametral compression until the failure of the specimen occurred. The mortar specimens were demolded 24 hours after casting. Subsequently, the geopolymer mortar specimens were cured under ambient laboratory conditions at a temperature of 27 ± 2 °C and a relative humidity of 60 ± 5% throughout the experimental period. In contrast, the OPC control specimens were cured by water immersion in accordance with the relevant standard procedures. The specified curing conditions were maintained consistently for all specimens until the designated testing ages of 7, 28, and 90 days, ensuring uniform curing throughout the study. Water absorption rate was studied using ASTM C642-21 [26], where specimens were immersed in water until saturation and percent mass increase was calculated as an absorption index. Chloride ion permeability was assessed according to rapid chloride permeability test (RCPT) method as per ASTM C1202-22 [27], which measured the total electrical charge passed through wetted discs under

60 volts DC for six hours. XRD analysis was conducted to investigate the mineral phases evolved during geopolymerization by analyzing an adequate 2θ range for crystalline and amorphous phases formed during geopolymerization process. SEM was used to determine the microstructure and porosity in the geopolymer matrix, while EDS technique in combination with SEM was utilized to detect the major elements (Si, Al, Ca, Na, and O).

5. RESULTS AND DISCUSSION

5.1 Compressive strength

Compressive Strength Results of Geopolymer Mortar Mixes vs. Conventional Cement Mortar Specimens at ages 7, 28, and 90 Days are illustrated in Figure 1 below. Four mortars were assessed in this study: 100% FA (F100), 100% Ground Granulated Blast Furnace Slag (G100), Binary Blended Mixture (F50G50), and Conventional Cement Mortar (C100). According to the experimental data, compressive strength test results demonstrate that all geopolymer mixtures show higher strength compared to conventional cement mortar throughout all testing times which confirms high efficiency of alkali activation technology to produce high-performance materials.

Compressive strength at age of 7 days was measured as 25.76 MPa for F100, 26.47 MPa for G100, 29.77 MPa for F50G50, and 23.33 MPa for C100. Comparing with C100 mortar mix, the improvements in compressive strength performance are 10.42%, 13.45%, and 27.60% for F100, G100, and F50G50 mortars, respectively. As seen from the obtained data, the highest compressive strength among three geopolymer mortar mixes was observed in case of binary mixture which means that the combination of FA and GGBS can significantly accelerate the process of geopolymerization, as well as strength development.

At age of 28 days, the compressive strengths reached 39.66 MPa for F100, 40.64 MPa for G100, 45.72 MPa for F50G50, and 35.53 MPa for C100. Comparing with the conventional cement mortar, the improvements in compressive strength are equal to 11.63%, 14.39%, and 28.68% for F100, G100, and F50G50 mortars, respectively. It may be assumed that the highest compressive strength performance at age of 28 days is explained by synergetic effect of FA and GGBS resulting in denser and more efficient geopolymeric matrix formed as a result of C-A-S-H and N-A-S-H gels production.

Comparative assessment of compressive strength at age of 90 days revealed that all geopolymer mortars continued strength development process. Compressive strengths at age of 90 days are 42.88 MPa for F100, 43.91 MPa for G100, 46.19 MPa for F50G50, and 38.52 MPa for C100. Comparing with the C100 mortar mixture, the improvements are 11.32%, 13.99%, and 19.91% for F100, G100, and F50G50, respectively. At later stages, improvements in compressive strength performance become slightly lower due to continuous hydration process which takes place in conventional cement mortar.

High compressive strength exhibited by geopolymer mortar, especially F50G50 mixture, is due to effective interaction between FA and GGBS in geopolymerization reactions. The source of silica and alumina is FA, whereas GGBS provides extra calcium that helps to increase dissolution of aluminosilicate compounds and form both N-A-S-H and C-A-S-H gels simultaneously. The reaction produces a denser structure with limited pore connectivity and strong interface bonding between binders and aggregates. As a result, cracks cannot easily occur within this matrix because it does not allow any crack development. Hence, this geopolymer mortar exhibits higher compressive strength than cement mortar.

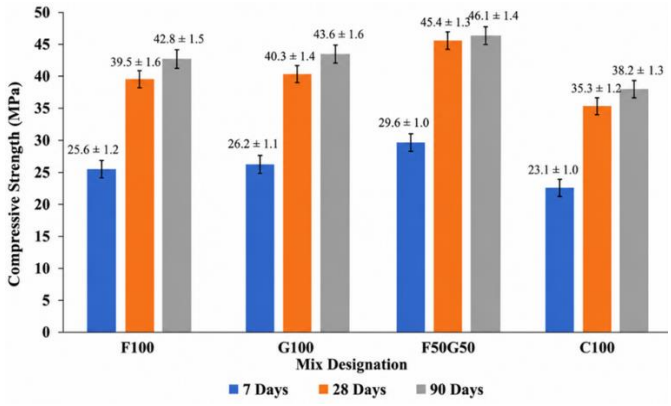

Figure 1. Results on compressive strength of mortar

5.2 Split tensile strength

Figure 2 shows the split tensile strength test results for geopolymer and conventional cement mortar samples cured for 7, 28, and 90 days. Four mortar mixtures are used to analyze the effect of binders on tensile strength development; these include mortar containing 100% FA (F100), 100% Ground Granulated Blast Furnace Slag (G100), 50% FA + 50% GGBS (F50G50), and conventional cement mortar (C100). It was determined that split tensile strength values for all geopolymer mortar mixtures exceed those for conventional cement mortar during the whole curing time, which proves the efficiency of using alkali-activated binders for improving tensile properties of concrete.

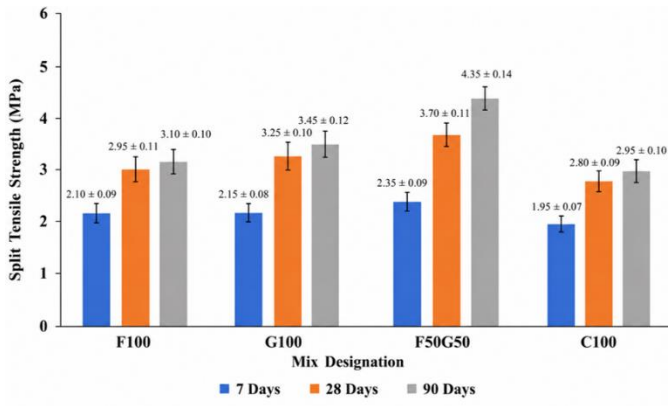

Figure 2. Results on split tensile strength of mortar

At 7-day curing, the obtained values of split tensile strength are as follows: 3.10 MPa (F100), 3.15 MPa (G100), 3.30 MPa (F50G50), and 2.85 MPa (C100). As compared to conventional cement mortar, split tensile strength increases by 8.77% for F100 mortar, 10.53% for G100, and 15.79% for F50G50. At early age, the greatest split tensile strength is exhibited by the binary geopolymer mix F50G50, which indicates that the presence of GGBS promotes quick bond formation due to the accelerated geopolymerization process.

At 28-day curing, the strength of geopolymer mortars

remained superior to the strength of the control mortar. The following values of split tensile strength were registered: 3.80 MPa (F100), 3.85 MPa (G100), 4.10 MPa (F50G50), and 3.55 MPa (C100). In comparison with the cement mortar, the split tensile strength increases by 7.04% for F100, 8.45% for G100, and 15.49% for F50G50. The significant performance improvement demonstrated by binary geopolymer mixture proves positive interactions between the reactants of this mixture, leading to dense matrix formation and effective stress transfer in mortar.

At 90-day curing, additional improvement in strength parameters was noted for all mixtures. The following split tensile strengths were registered: 3.95 MPa (F100), 4.15 MPa (G100), 4.85 MPa (F50G50), and 3.65 MPa (C100). As compared to conventional cement mortar, split tensile strength increases by 8.22% for F100, 13.70% for G100, and 32.88% for F50G50. Such a strong increase in tensile strength for the F50G50 binary mix proves positive impact of interaction between FA and GGBS on continuous formation of geopolymer gels in the matrix.

From the analysis of all test results, it can be concluded that geopolymer mortar specimens demonstrate superior split tensile strength as compared to conventional mortar at different curing ages. Moreover, among all mortar mixtures tested, the best performance in terms of split tensile strength is provided by F50G50 binary mortar, followed by G100 and F100. Geopolymer mortar is characterized by superior tensile strength as compared to conventional mortar, which is explained by the high degree of polymerization of matrix.

Superior tensile strength performance of geopolymer mortar is conditioned by the polymerization of aluminum-silicon structure that develops during geopolymerization process. While FA is characterized by a high content of reactive silicon and aluminum oxides, GGBS provides the source of calcium. Under alkali activation, both N-A-S-H and C-A-S-H gels form in the matrix, contributing to the development of good bond with fine aggregate particles, minimizing porosity, and limiting microcrack formation under tensile loading.

5.3 Water absorption test

The results of water absorption analysis of geopolymer and conventional cement mortar samples are provided in Figure 3.

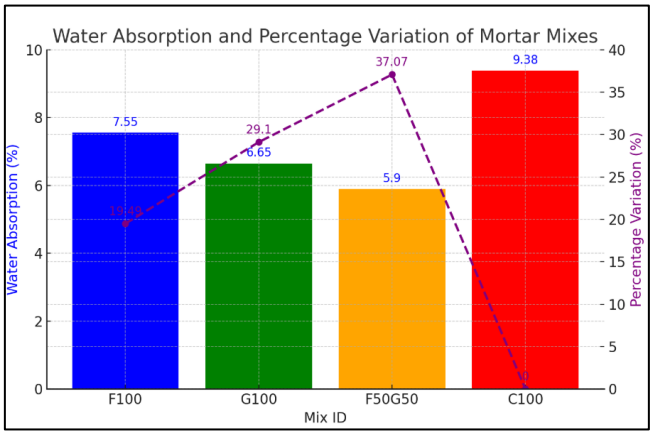

Figure 3. Results on water absorption test on mortar mixes

It should be noted that water absorption is one of the critical durability characteristics of mortars and reflects its porosity and permeability; thus, the lower value of this property implies higher durability of mortar. As can be seen from Figure 3, conventional cement mortar (sample C100) had the highest water absorption rate equal to 9.38%. All analyzed geopolymer mixtures were characterized by significantly lower water absorption than sample C100. Sample F100 had water absorption equal to 8.55%, which corresponded to 8.85% decrease compared with the conventional cement mortar sample. Mortar G100 showed the reduction in water absorption up to 6.65%, i.e., 29.10% decrease. The lowest level of water absorption was observed in the case of geopolymer mixture consisting of two components in 50-50 ratio (F50G50), which demonstrated water absorption equal to 5.90%, i.e., 37.10% (approximately 38.07%) decrease in comparison with C100. These results prove the fact that the use of FA and GGBS as the partial substitutes of cement provides significant improvements in mortar durability; moreover, the usage of both FA and GGBS as geopolymer raw materials leads to even higher increase in impermeability.

It can be stated that the low water absorption of geopolymer mortars is due to their highly dense structure, which results from the process of geopolymerization. Thus, FA provides reactive SiO2 and Al2O3, the elements necessary for the synthesis of N-A-S-H gel, whereas GGBS serves as the source of reactive Ca, contributing to the synthesis of C-A-S-H gel. Therefore, the presence of both binding gels contributes to the filling of pores within the matrix, its refinement, and enhancement of interfacial transition zone strength. The lowest water absorption in sample F50G50 can be explained by the interaction of FA and GGBS during geopolymerization leading to the formation of the highly dense geopolymer matrix with reduced number of pores. Conventional cement mortar contains larger pores formed during the process of cement hydration. Consequently, the low water absorption of geopolymer mortars proves the higher durability of such material.

5.4 Rapid chloride permeability test

Results of RCPT conducted on geopolymer and traditional cement mortars at 7, 28, and 90 days are provided in Figure 4. Lower charge passed through the mortar indicates a more durable material that provides better resistance to reinforcement corrosion due to chloride ion penetration. The conventional cement mortar (C100) showed the highest permeability at all ages – 3812 Coulombs (C) at 7 days, 3211 C at 28 days, and 2553 C at 90 days. High permeability indicates the relatively large number of pores in this material due to which it provides poor resistance to chloride ions penetration. On the other hand, geopolymer mortars revealed very low permeability at all curing ages.

Thus, at 7 days of curing, the F100, G100, and F50G50 mixtures had the following permeabilities: 2111, 1558, and 1189 C, correspondingly. In comparison to C100, the permeability was reduced by 44.62%, 59.13%, and 68.81% for the aforementioned geopolymer mortars. The binary geopolymer mixture (F50G50) was shown to possess the lowest permeability at an early age of curing, thus indicating intensive formation of the geopolymer gel.

Further reduction in chloride permeability was observed at 28 days of curing: it was equal to 1645 C for F100, 1138 C for G100, and 1332 C for F50G50, thus decreasing permeability by 48.77%, 64.56%, and 58.52% compared to conventional cement mortar. Although F50G50 demonstrated slightly higher chloride permeability in comparison to G100 mortar, it

still provided good resistance to chloride ions, as indicated by relatively low permeability compared to C100.

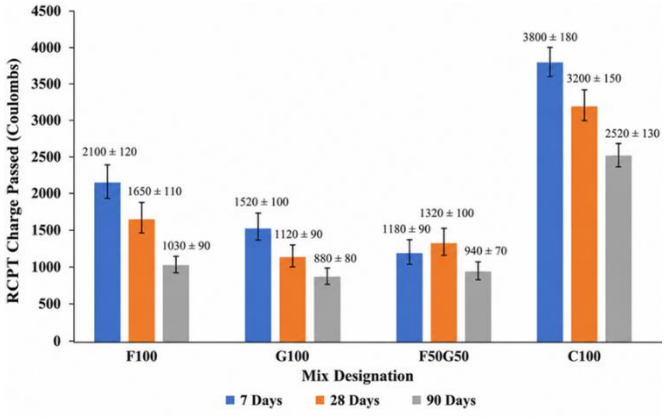

Figure 4. Rapid chloride permeability test (RCPT) results on mortar mixes

Continued development of geopolymerization process significantly improved chloride resistance at 90 days of curing. Thus, permeabilities were 1048, 889, 947, and 2553 C for F100, G100, F50G50, and C100, correspondingly. In comparison to conventional cement mortar, permeability was reduced by 58.95%, 65.18%, and 62.91% for the F100, G100, and F50G50 samples, correspondingly. Geopolymer mortar G100 showed the lowest permeability at a late age of curing, while both G100 and F50G50 mixtures provided low permeability, thus ensuring excellent long-term durability.

In summary, the results of RCPT tests show that the geopolymer mortars provide considerably higher resistance to chloride ions penetration at all curing ages. Application of FA and GGBS allowed reducing chloride permeability by providing a highly dense material and thus reducing capillary pores connectivity. G100 and F50G50 were the most durable materials and showed the best durability performance. Thus, geopolymer mortars can be successfully used in environments exposed to chlorides and requiring high durability and resistance to chloride-induced corrosion.

High chloride resistance of geopolymer mortars is associated with the process of aluminosilicate gel formation, which results in highly dense and inter-connected network of solid particles in the material. Due to incorporation of FA, geopolymer mortar contains large amounts of silica and alumina forming (N-A-S-H) gel. In addition, GGBS provides calcium oxide necessary for the formation of calcium aluminosilicate hydrate gel (C-A-S-H), thus providing double benefits to the durability of the material. Due to the presence of two gel types in the material, pores are refined and their connectivity is minimized, which in turn minimizes permeability. Therefore, fewer opportunities are available for the ingress of chloride ions. Moreover, due to higher amount of calcium oxide, geopolymerization takes place rapidly, and consequently, the structure is formed tighter and provides lower permeability at early ages of curing.

5.5 X-ray diffraction analysis

The XRD pattern for the F50G50 geopolymer mortar is shown in Figure 5. Diffractogram reveals the presence of several crystalline phases, such as Portlandite ($Ca(OH)_2$), Quartz (SiO_2), Belite (C_2S), Alite (C_3S), Mullite ($Al_6Si_2O_{13}$), and iron-containing compounds due to the multimineralogical composition of the geopolymer material. The most prominent diffractogram peak belongs to Portlandite and corresponds to $2\theta = 31°$ (d = 1.372 Å). Prominent peaks belonging to Quartz can be seen near $2\theta = 27°$ (d = 2.109 Å) and $2\theta = 28°$ (d = 2.119 Å). Belite is characterized by two peaks around $2\theta = 35°$ and $2\theta = 36°$ (d ~ 2.196 Å). Additional minor peaks for Alite, Mullite, and iron-containing compounds were found in the high-angle range of diffraction. The presence of the relatively broad hump in the background of the XRD pattern indicates that an amorphous aluminosilicate gel was formed, which is a clear indication of geopolymerization processes.

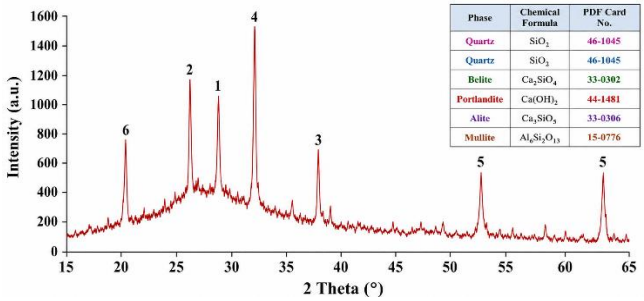

Figure 5. X-ray diffraction (XRD) analysis of geopolymer mortar

Superior characteristics of the F50G50 geopolymer mortar are attributed to interactions between FA and GGBS particles when subjected to alkali activation. Silica and alumina oxides from FA dissolve in alkali solution and form N-A-S-H gel, while calcium from GGBS helps in the synthesis of C-A-S-H gel. The combination of these gels creates a strong binding network and allows filling of capillary pores and increasing the densification of the matrix. Quartz provides relatively inert filler phase with better particle packing, while Mullite is thermally stable because of its chemical inertness. Presence of Belite and Alite helps to provide additional calcium for the formation of C-A-S-H gel. Thus, the combination of these crystalline phases together with the major component – geopolymer gel – improves the pore structure of the matrix, increases binding, reduces microcracking, and enhances compressive strength.

5.6 Scanning electron microscopy and energy-dispersive spectroscopy analysis

SEM coupled with EDS was performed to study the morphology, geopolymerization level, porosity, and chemical composition of F50G50 geopolymer mortar. Different SEM images were captured at varying levels of magnification in order to examine the microstructure of geopolymeric gel and distribution of unreacted precursor particles whereas EDS was used to detect the main elements participating in the geopolymerization process. Figure 6 and Figure 7 represent SEM micrographs with the corresponding EDS spectra.

SEM microscopy with a magnification of 500× (Figure 6) shows a dense microstructure of the geopolymer matrix. The matrix includes partially geopolymerized FA and other particles embedded in the homogenous and compact continuous aluminosilicate gel matrix. It is observed that some spherical-shaped FA particles are still visible due to incomplete dissolution of precursor particles. Such particles serve as micro-fillers and continue to take part in the geopolymerization process at advanced ages of curing. In addition, it can be noted that there are no cracks inside the

geopolymer matrix. This observation proves the formation of the stable geopolymeric network capable of preventing the formation and further development of cracks.

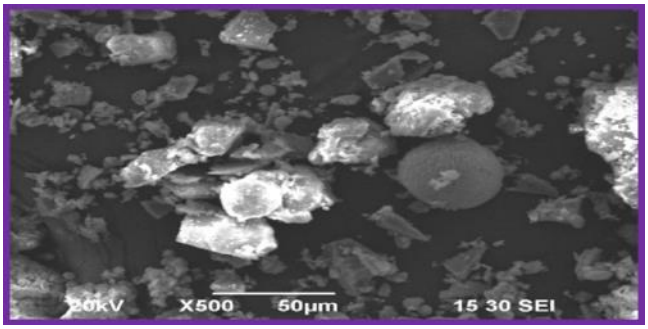

Figure 6. Scanning electron microscopy (SEM) image of geopolymer mortar

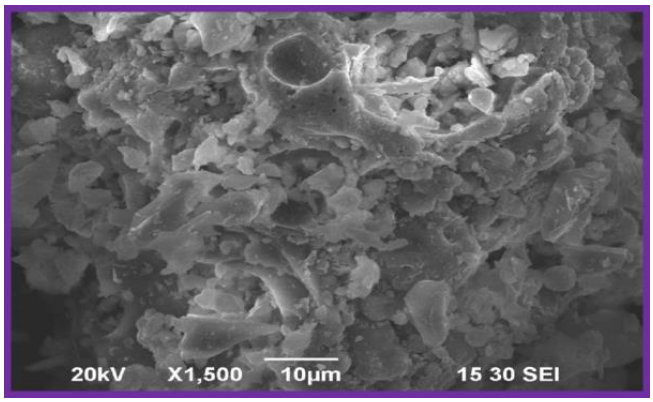

Figure 7. Geopolymer coexistence and C–S–H phase in Geopolymer

Microstructure of F50G50 geopolymer mortar is shown at the magnification of 1500× (Figure 7). The microstructure comprises a compact geopolymer matrix composed of dense geopolymeric reaction products and only a few isolated pores. It can be noticed that geopolymeric matrix contains two types of reaction products: calcium-rich and aluminosilicate. The presence of such reaction products suggests that C-A-S-H and N-A-S-H gels formed during geopolymerization process due to the combination of GGBS and FA. Thus, the continuous matrix of geopolymeric products encapsulates remaining unreacted precursor particles, limiting pores, and increasing porosity.

In order to investigate the chemical composition of geopolymer mortar, energy-dispersive x-ray spectroscopy analysis was used. The results of elemental composition analysis are represented in Figure 8. According to EDS, the geopolymer matrix consists of silicon, oxygen, and aluminum that correspond to aluminosilicate matrix. However, there are some other elements, including sodium, calcium, magnesium, sulfur, titanium, potassium, and iron. The presence of sodium proves the use of an alkaline solution for geopolymerization. Calcium comes from GGBS and serves as an additional component participating in C-A-S-H gel formation. Thus, the combination of Si, Al, and Ca confirms the creation of a hybrid gel that includes N-A-S-H and C-A-S-H gels.

Table 2 contains quantitative data obtained using EDS analysis. As can be seen from Table 2, oxygen is the predominant element in terms of mass percentage. Silicon and aluminum are also abundant elements in terms of chemical composition due to the aluminosilicate framework formation. High silicon content suggests extensive polymerization of silica precursors, whereas aluminum contributes to the formation of three-dimensional geopolymeric frameworks. Detected calcium leads to geopolymer matrix densification due to secondary gel formation. Magnesium, sulfur, potassium, titanium, and iron are trace amounts of minerals from FA and GGBS that have a minor influence on geopolymerization process.

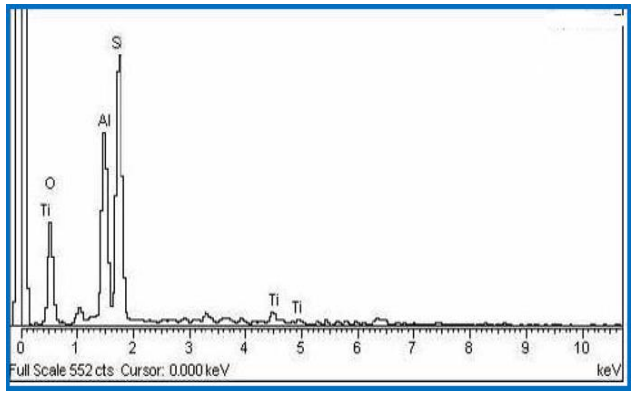

Figure 8. Energy-dispersive spectroscopy (EDS) spectrum of geopolymer mortar

Table 2. Contents of geopolymer mortar using energy-dispersive spectroscopy (EDS)

Element	Weight%	Atomic%
O	47	66.9
Na	6.74	5.87
Mg	0.58	0.48
Al	9.35	8.19
Si	24.35	18.35
S	0.34	0.21
K	0.84	0.45
Fe	10.69	1.00
Total	100	100

In conclusion, it is possible to state that SEM and EDS analyses reveal that the geopolymer matrix is dense, compact, and homogeneous due to limited pore structure and well-developed geopolymeric gel. The interaction of FA and GGBS leads to the formation of N-A-S-H and C-A-S-H gels, providing enhanced properties. Improved mechanical properties, low water absorption, decreased chloride permeability, and increased sliding tensile and compressive strength prove the feasibility of F50G50 formulation.

6. CONCLUSIONS

This research focused on assessing the effect of FA, GGBS, and their combination on the properties of geopolymer mortar using a total replacement of OPC. The following conclusions can be derived from the experiments:

- All of the tested mixtures of geopolymer mortars provided better technical characteristics in comparison with the OPC mortar throughout the whole curing period. This finding proved the efficiency of the alkaline activation method in producing environmentally friendly construction materials.
- The best results concerning compressive strength were achieved by the F50G50 binary geopolymer mortar

composition reaching its peak at 90 days with the maximum value of 46.19 MPa. This mixture showed approximately 19.91% higher strength than the control sample due to the synergy between FA and GGBS.

- The trend in splitting tensile strength was analogous to the previous characteristic. As for the highest values of the studied parameter, the record was achieved by the F50G50 sample at 90 days amounting to 4.85 MPa. In other words, it had about 32.88% more tensile strength than the control one thanks to the densified geopolymer structure and improved bond between the matrix and aggregates.
- Regarding the durability, geopolymer mortars provided much lower water absorption levels and chloride permeability in comparison with the traditional Portland cement mortar samples. Particularly, the F50G50 composition had around 38% lower water absorption. The lowest chloride permeability level was also recorded by the F50G50 sample, decreasing by almost 63% relative to the control sample.
- The analysis of XRD patterns confirmed the successful formation of the geopolymer matrix via the presence of amorphous phases of aluminosilicates and crystalline minerals like quartz, mullite, and calcium-containing compounds. It resulted in the formation of a stable, mechanically strong matrix of geopolymer mortar.
- The SEM images presented a denser, uniform, and well-formed microstructure characterized by reduced number of capillary pores and microcracks. Moreover, EDS analysis revealed the high content of such elements as silicon, aluminum, oxygen, and calcium, which were the major components of the geopolymer mortar. As for the densification mechanism, the main role was played by N-A-S-H and C-A-S-H gels.
- Consequently, a combination of FA and GGBS provided a geopolymer mortar with improved strength and durability properties and optimized microstructure. Therefore, this binary geopolymer system could be considered as the most sustainable solution compared to other investigated options and the traditional cement.

In conclusion, FA-GGBS geopolymer mortar is a promising environmentally friendly alternative to conventional cement mortar with enhanced mechanical properties and low water absorption and chloride permeability.

REFERENCES

[1] Vijay, K., Sarma, V.V.S., Kuruva, V., Kumar, A.U., Detu, K., Reddy, P.N. (2026). A bio-polymeric strategy for enhancing the strength, durability of concrete and shrinkage reduction. Scientific Reports, 16(1): 11346. https://doi.org/10.1038/s41598-026-38804-0

[2] Reddy, G.G.K., Reddy, A.N., Sankar, B., Reddy, P.N. (2026). Assessment of flexural behavior and numerical simulation of UHPFRC beams with steel fibers. Iranian Journal of Science and Technology, Transactions of Civil Engineering, 50(1): 787-799. https://doi.org/10.1007/s40996-025-01844-z

[3] Reddy, P.N., Kavyatheja, B.V., Hussain Vali, R., Madhu Mohan, G., Damodhara Reddy, B., Aruna Jyothy, S., Mohan Babu, M. (2023). Predicting the strength properties of LWC using response surface. In International Conference on Intelligent Manufacturing and Energy Sustainability, pp. 505-515. https://doi.org/10.1007/978-981-99-6774-2_45

[4] Damodhara Reddy, B., Narasimha Reddy, P., Aruna Jyothy, S., Mohan Babu, M., Venkata Kavyatheja, B. (2023). Predicting compressive strength of self-repairing concrete using artificial neural networks. In International Conference on Intelligent Manufacturing and Energy Sustainability, pp. 495-504. https://doi.org/10.1007/978-981-99-6774-2_44

[5] Ashok Kumar, M., Vijay, K., Syam Babu, D., Reddy, P.N., Sagar, T.S. (2024). Feasible study on optimal utilization of blended fly ash and GGBS on the performance of concrete. Journal of Physics: Conference Series, 2779(1): 012007. https://doi.org/10.1088/1742-6596/2779/1/012007

[6] Davidovits, J. (1991). Geopolymers: Inorganic polymeric new materials. Journal of Thermal Analysis and Calorimetry, 37(8): 1633-1656. https://doi.org/10.1007/bf01912193

[7] Davidovits, J. (2013). Geopolymer cement. A review. Geopolymer Institute, Technical Papers, 21: 1-11.

[8] Hardjito, D., Wallah, S.E., Sumajouw, D.M., Rangan, B.V. (2004). On the development of fly ash-based geopolymer concrete. Materials Journal, 101(6): 467-472.

[9] Hardjito, D., Rangan, B.V. (2005). Development and properties of low-calcium fly ash based geopolymer concrete (Research Report GC1). Curtin University of Technology.

[10] Provis, J.L., van Deventer, J.S.J. (2009). Geopolymers: Structure, Processing, Properties and Industrial Applications. Woodhead Publishing. https://doi.org/10.1533/9781845696382

[11] Provis, J.L., Bernal, S.A. (2014). Geopolymers and related alkali-activated materials. Annual Review of Materials Research, 44(1): 299-327. https://doi.org/10.1146/annurev-matsci-070813-113515

[12] Bernal, S.A., Provis, J.L., Walkley, B., San Nicolas, R., et al. (2013). Gel nanostructure in alkali-activated binders based on slag and fly ash, and effects of accelerated carbonation. Cement and Concrete Research, 53: 127-144. https://doi.org/10.1016/j.cemconres.2013.06.007

[13] Nath, P., Sarker, P.K. (2014). Effect of GGBFS on setting, workability and early strength properties of fly ash geopolymer concrete cured in ambient condition. Construction and Building Materials, 66: 163-171. https://doi.org/10.1016/j.conbuildmat.2014.05.080

[14] Hu, Y., Tang, Z., Li, W., Li, Y., Tam, V.W. (2019). Physical-mechanical properties of fly ash/GGBFS geopolymer composites with recycled aggregates. Construction and Building Materials, 226: 139-151. https://doi.org/10.1016/j.conbuildmat.2019.07.211

[15] Bellum, R.R., Muniraj, K., Madduru, S.R.C. (2020). Exploration of mechanical and durability characteristics of fly ash-GGBFS based green geopolymer concrete. SN Applied Sciences, 2(5): 919. https://doi.org/10.1007/s42452-020-2720-5

[16] Rajini, B., Narasimha Rao, A.V., Sashidhar, C. (2021). Micro-level studies of fly ash and GGBS—Based geopolymer concrete using SEM and XRD. IOP Conference Series: Materials Science and Engineering, 1130(1): 012062. https://doi.org/10.1088/1757-899X/1130/1/012062

[17] Škvára, F., Kopecký, L., Nemecek, J., Bittnar, Z.D.E.N.I.K. (2006). Microstructure of geopolymer

materials based on fly ash. Ceramics-Silikaty, 50(4): 208-215.
[18] Taylor, H.F. (1997). Cement Chemistry. Thomas Telford.
[19] IS 12269. (2013). Ordinary Portland Cement, 53 Grade—Specification. https://infralens.in/code/IS-12269-2013.
[20] IS 3812 (Part 1). (2013). Pulverized Fuel Ash - Specification - Part 1: For use as pozzolana in cement, cement mortar and concrete. https://infralens.in/code/IS-3812-Part-1-2013.
[21] ASTM C989/C989M-18. (2018). Standard Specification for Slag Cement for Use in Concrete and Mortars. https://standards.iteh.ai/catalog/standards/astm/a24280f0-7b8c-4b1d-af2d-4390a93ef5b7/astm-c989-c989m-18a?srsltid=AfmBOoqw0e1fhufg0AC2t_1gDU-i6PAEbatWQJLej6QSZ0WqUUTLohmG.
[22] IS: 383. (2016). Coarse and Fine Aggregate for Concrete-Specification. https://www.services.bis.gov.in/tmp/tbl5_2024-11-10_11.pdf.
[23] IS: 9103. (2016). Admixtures for Concrete – Specification. https://infralens.in/code/IS-9103-2016.
[24] IS 516 (Part 1/Sec 1). (2021). Methods of Tests for Strength of Concrete - Part 1: Hardened Concrete - Section 1: Compressive, Flexural and Split Tensile Strength. https://infralens.in/code/IS-516-Part-1-Sec-1-2021.
[25] IS 5816. (1999). Method of Test Splitting Tensile Strength of Concrete. https://infralens.in/code/IS-5816-1999.
[26] ASTM C642-21. (2021). Standard Test Method for Density, Absorption, and Voids in Hardened Concrete.
[27] ASTM C1202-22. (2022). Standard Test Method for Electrical Indication of Concrete's Ability to Resist Chloride Ion Penetration.